

# Thermoelectrically cooled quantum-cascade-laser-based sensor for the continuous monitoring of ambient atmospheric carbon monoxide

Anatoliy A. Kosterev, Frank K. Tittel, Rüdiger Köhler, Claire Gmachl, Federico Capasso, Deborah L. Sivco, Alfred Y. Cho, Shawn Wehe, and Mark G. Allen

We report the first application of a thermoelectrically cooled, distributed-feedback quantum-cascade laser for continuous spectroscopic monitoring of CO in ambient air at a wavelength of 4.6  $\mu\text{m}$ . A noise-equivalent detection limit of 12 parts per billion was demonstrated experimentally with a 102-cm optical pathlength and a 2.5-min data acquisition time at a 10-kHz pulsed-laser repetition rate. This sensitivity corresponds to a standard error in fractional absorbance of  $3 \times 10^{-5}$ . © 2002 Optical Society of America  
OCIS codes: 280.1120, 280.3420, 300.6360.

Carbon monoxide (CO) is a regulated criteria pollutant that is produced by the incomplete combustion of carbon-based fuels that are widely used for power generation, industrial heating, petrochemical refining, and propulsion. The current method approved by the Environmental Protection Agency for continuous monitoring of ambient CO is nondispersive infrared technology, which is generally limited in sensitivity to  $>1$  parts per million, requires sample gas pretreatment, and has response times on the order of 30 s. The availability of portable, high-speed CO sensors with  $<100$ -parts per billion (ppb) sensitivity would provide better source apportionment and control of CO emissions. In this paper, we report the first application of a quantum cascade distributed feedback (QC-DFB) laser<sup>1,2</sup> toward this end. A pulsed, thermoelectrically cooled QC-DFB laser operating at 4.6  $\mu\text{m}$  (Ref. 3) was used to probe isolated

absorption transitions in the fundamental CO vibrational band.

A schematic of the sensor is shown in Fig. 1. We utilized the same quantum cascade laser housing that was used in our earlier work for ammonia detection.<sup>4</sup> The laser was mounted on a three-stage thermoelectric cooler that enabled us to set its substrate temperature anywhere above  $-55$  °C. An aspheric ZnSe collimation lens ( $f = 3$  mm, diameter = 6 mm) with antireflection (AR) coating for the  $\lambda = 8\text{--}12$   $\mu\text{m}$  spectral range used in Ref. 4 was replaced with a similar lens AR coated for  $\lambda = 3\text{--}12$   $\mu\text{m}$ . Furthermore the ZnSe housing window with a  $8\text{--}12\text{-}\mu\text{m}$  AR coating was replaced with an uncoated  $\text{CaF}_2$  window (30 arc min wedged). The main sensitivity-limiting factor in Ref. 4 was the pulse-to-pulse fluctuations of the laser energy. To overcome this limitation, we utilized a two-channel scheme. The IR beam was split into two paths by an uncoated 30 arc min wedged ZnSe plate. One part of the laser radiation was directed to the reference detector, and another part through a gas cell to the signal detector. Both detectors were liquid-nitrogen-cooled photovoltaic HgCdTe devices (Kolmar Technologies, KMPV8-1-J1/DC). The gas cell was fabricated from a 19-mm-diameter glass tube. One end of the cell was equipped with an uncoated 30' wedged  $\text{CaF}_2$  window and the other end with a mirror, resulting in a two-pass configuration with a total optical pathlength of 102 cm.

The QC-DFB laser was operated according to the

---

A. A. Kosterev (akoster@rice.edu) and F. K. Tittel are with the Rice Quantum Institute, Rice University, Houston, Texas 77251-1892. At the time of this research, R. Köhler, C. Gmachl, F. Capasso, D. L. Sivco, and A. Y. Cho are with Bell Laboratories, Lucent Technologies, 600 Mountain Avenue, Murray Hill, New Jersey 07974. S. Wehe and M. G. Allen are with the Physical Sciences Inc., 20 New England Business Center, Andover, Massachusetts 01810. R. Köhler is now with Scuola Normale Superiore, Pisa, Italy.

Received 5 October 2001.

0003-6935/02/061169-05\$15.00/0

© 2002 Optical Society of America

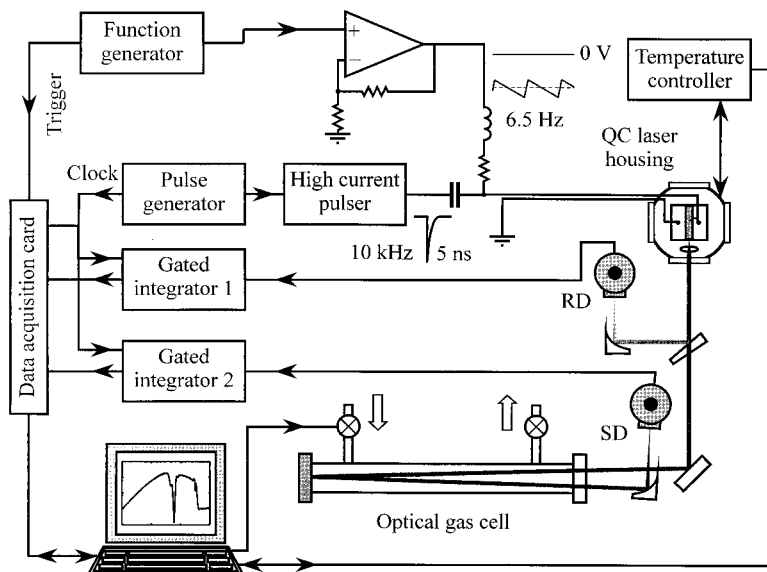


Fig. 1. Schematic of the CO gas sensor based on a thermoelectrically cooled pulsed QC-DFB laser. RD, SD—reference and signal IR detectors, respectively.

procedures described in Refs. 4–6. Briefly, the laser was excited by  $\sim 5$ -ns long,  $\sim 20$  A peak current pulses at a repetition rate of 10 kHz. A sawtooth-modulated subthreshold current was added to the excitation pulses in order to tune the laser wavelength. The modulation frequency was set to 6.5 Hz so that  $\sim 1500$  laser pulses were generated during one period. The average laser substrate temperature was maintained at  $-23.3$  °C. With the appropriate settings of the quantum cascade laser temperature and current, the laser frequency could be tuned over a  $0.41\text{-cm}^{-1}$  region encompassing the R(3) absorption line at  $2158.300\text{ cm}^{-1}$ . This transition is free from interferences from atmospheric species such as  $\text{H}_2\text{O}$ . The laser frequency scan was calibrated with interference fringes from an uncoated ZnSe air-gap etalon with a free spectral range (FSR) of  $0.030\text{ cm}^{-1}$  (Fig. 2). The deviation from a linear fit did not exceed  $\pm 0.08$  FSR, or  $2.4 \times 10^{-3}\text{ cm}^{-1}$  in the region between the 250th and 1100th pulse, which was used in data processing. This small nonlinearity was ignored in the data analysis. Absolute frequency assignment was performed by comparison of experimental absorption spectra of CO and  $\text{N}_2\text{O}$  with the HITRAN96 database.<sup>7</sup>

The time response of the HgCdTe detectors was  $\sim 35$  ns. The peak intensity of each pulse was measured with two gated integrators (one for each detector) with an integration window set to  $\sim 15$  ns, and subsequently digitized (simultaneously for each detector) with a 16-bit data acquisition card (National Instruments, DAQCard-AI-16XE-50). Each frequency sweep consisted of 1500 laser pulses at a 10-kHz repetition rate; both the repetition rate and the number of pulses in a scan are limited by the technical characteristics of the particular data-acquisition card used in the present experiment. Air was sampled automatically into the gas cell

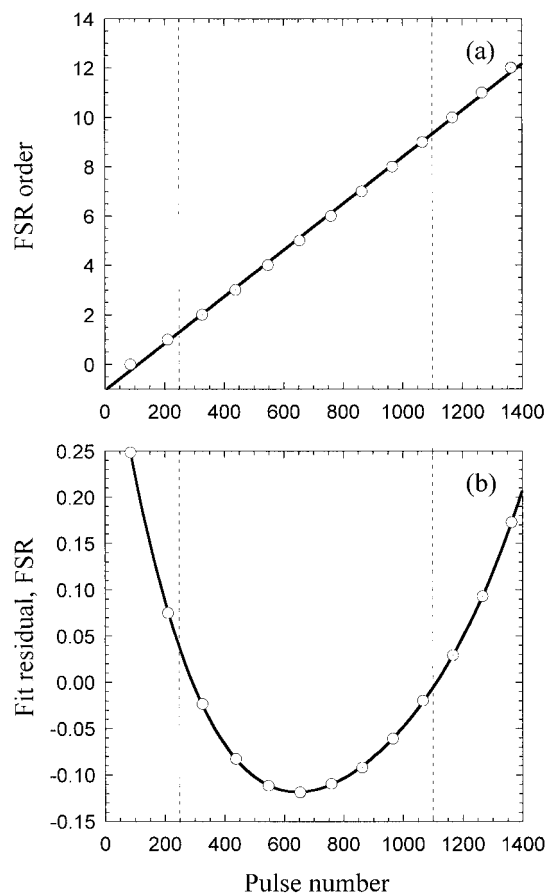


Fig. 2. Laser scan calibration with an air-gap etalon formed by two uncoated ZnSe surfaces, FSR of  $0.030\text{ cm}^{-1}$ . Horizontal axis is a laser pulse number in the frequency scan. (a) Peaks of etalon interference fringes. Vertical axis is a relative FSR order, and the solid curve shows best linear fit. (b) Residual of the linear fit. Solid curve is the best fourth-order polynomial fit of the residual. The region between the two dashed vertical lines was used in the absorption data analysis.

through a computer-controlled valve and a pressure controller that ensured constant pressure of 95 torr during the data-acquisition process.

Each cycle of the spectral data acquisition consisted of the following steps:

1. Initially, a spectral baseline was acquired by use of a preset number of the laser-frequency sweeps (500 in most of our measurements) while the cell was evacuated;  $i$ th pulse of  $k$ th sweep provided one  $i$ th data point each for signal and reference channels. Then the data were averaged over all  $k$ 's for each  $i$ , resulting in two arrays  $\mathbf{IR}_e$  and  $\mathbf{IS}_e$  of 1500 elements each.

2. The same measurements were carried out with 95 torr of ambient air in the cell, yielding the arrays  $\mathbf{IR}_a$  and  $\mathbf{IS}_a$ .

3. The laser beam was then blocked by means of a computer-controlled flipper, and offset voltages OffR and OffS were measured for each channel; these offset voltages come from the gated integrators and slowly drift in time.

4. The measured offset was subtracted from the previously acquired data, and the ratio  $\mathbf{R} = (\mathbf{IS} - \text{OffS})/(\mathbf{IR} - \text{OffR})$  was calculated for each data point  $i$  in the respective arrays.

The net absorption spectrum was found from the offset-corrected data as  $\mathbf{A} = (\mathbf{R}_a - \mathbf{R}_e)/\mathbf{R}_e$  and the baseline of this data set was forced to zero through subtraction of a polynomial best fit.

The laser line was found to have an asymmetric shape and a FWHM of  $\sim 0.02 \text{ cm}^{-1}$ , comparable with the CO absorption line width of  $0.018 \text{ cm}^{-1}$  at 95 torr air pressure. To extract the CO concentration from this kind of spectral data we used the same procedure as described in Ref. 4. Namely,

1. A reference low-noise spectrum was acquired with a  $\sim 0.08\%$  CO in-air mixture at 95 torr in a 3-cm-long gas cell (peak absorption  $\sim 9\%$ ). The actual concentration of CO in the reference sample was determined through comparison of the integrated absorbance ( $\int \alpha d\nu$ , where  $\alpha [\text{cm}^{-1}]$  is the absorption coefficient) to the area predicted by HITRAN96 database for the same temperature. The spectrum was stored in computer memory as a function  $y_i = f(i)$ , where  $i$  is the data point index.

2. The concentration of CO in ambient-air samples was then determined by the best-fit coefficients of the acquired absorption spectrum to the reference CO lineshape by use of the function

$$y_i = Cf(i - x) + b. \quad (1)$$

Here, the parameter  $C$  is proportional to the CO concentration in the investigated sample and  $b$  is a measure of the baseline drift.

An example absorption spectrum acquired as described above by use of 500 laser-sweep averages for each of an evacuated and air-filled measurement (total of 1000 scans, i.e., 2.5 min data acquisition time)

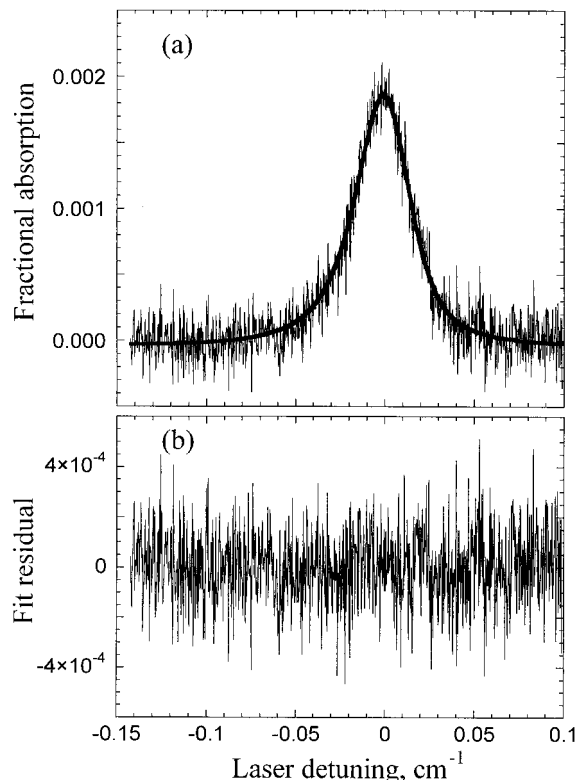


Fig. 3. (a) An example of the CO absorption detected in ambient air; the data are fitted using Eq. (1). (b) Fit residual.

is shown in Fig. 3(a), along with the best-fit line. From the fit residual shown in Fig. 3(b) a single-point standard deviation in measured fractional absorbance is  $\sigma = 1.5 \times 10^{-4}$ . The noise originated primarily from the gated integrators and did not change when the laser radiation was blocked. The line center in our experiments [parameter  $x$  in Eq. (1)] exhibited a small slow drift caused by slight drift of the laser temperature over measurement time, and  $b$  was always close to zero. With a simplifying assumption that  $x \equiv 0$  and  $b \equiv 0$  the error analysis developed in Ref. 8 can be applied, and a standard deviation  $\delta A$  of the measured absorption line area  $A$  is given by

$$\delta A = \sigma \left[ \frac{\Delta\nu}{\int g^2(\nu) d\nu} \right]^{1/2}, \quad (2)$$

where  $\Delta\nu$  is the frequency scan resolution and  $g(\nu)$  is the absorption spectrum normalized by the condition  $\int g(\nu) d\nu = 1$ . In our experiments, the spectral separation of the data points was  $\Delta\nu = 2.9 \times 10^{-4} \text{ cm}^{-1}$ , and a numerical integration of the acquired lineshape resulted in  $\int g^2(\nu) d\nu = 13.4 \text{ cm}$ . This yields  $\delta A = 7.14 \times 10^{-7} \text{ cm}^{-1}$  (corresponding to a peak absorption  $1.5 \times 10^{-5}$ ) when these numbers are substituted in Eq. (2), which, for a pathlength of 102 cm and the selected CO absorption line, translates into a noise-equivalent detection limit of  $\delta[\text{CO}] = 6.5 \text{ ppb}$ .

To verify this predicted accuracy and the long-term

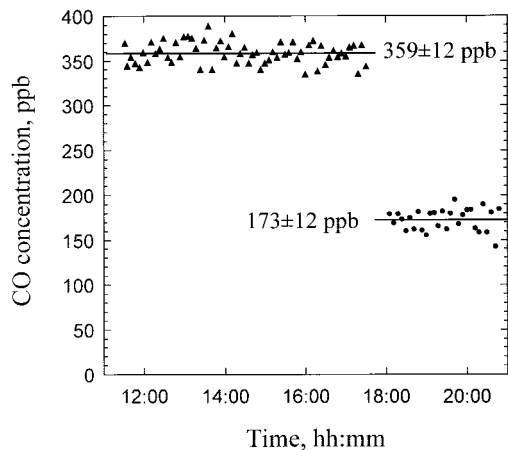


Fig. 4. CO concentration measured in the gas from different sources: a cylinder with UHP grade of  $N_2$ -triangles and a cylinder with rural US mountain air sample-circles. The measurements were performed every six minutes.

stability of the system, we performed a continuous run of measurements when the gas was sampled sequentially from a cylinder containing ultra-high priority grade  $N_2$  and a second cylinder containing Niwot Ridge, Colorado mountain air provided by the National Oceanic and Atmospheric Administration.<sup>9</sup> As shown in Fig. 4, the average measured concentration remained stable for the duration of the first run of measurements (5 hours), and the scattering of results indicate  $\delta[CO] = 12$  ppb for both cylinders (corresponding to standard error in peak absorption of  $3 \times 10^{-5}$ ). The slight decrease in the actual precision of the sensor compared with the theoretical prediction is tentatively attributed to the laser frequency drift and imperfect baseline correction excluded from our simplified analysis by setting  $x$  and  $b$  to zero.

The CO sensor was also applied to continuous monitoring of the CO concentration in the ambient laboratory air. As evident in Fig. 5, two characteristic maxima of CO concentration were observed during a typical day, corresponding to morning and evening rush hour traffic. The short duration behavior of these broad maxima, however, was connected closely with local meteorological conditions, such as wind. A similar temporal behavior was observed in December 1996 when monitoring the CO concentration in laboratory air using midinfrared spectroscopy that is based on laser difference-frequency generation (see Fig. 8 in Ref. 10).

To improve the QC-DFB laser-based gas-sensor performance, we plan to upgrade the high-amplitude pulsed current source and data-acquisition electronics to enable a 1-MHz current pulse and data-sampling repetition rate. The data acquisition that now takes 2.5 min in our experiments would take only 1.5 s after such an upgrade. It is also possible to replace liquid-nitrogen-cooled detectors with the thermoelectrically cooled detectors to completely avoid the use of consumables in such gas sensors.

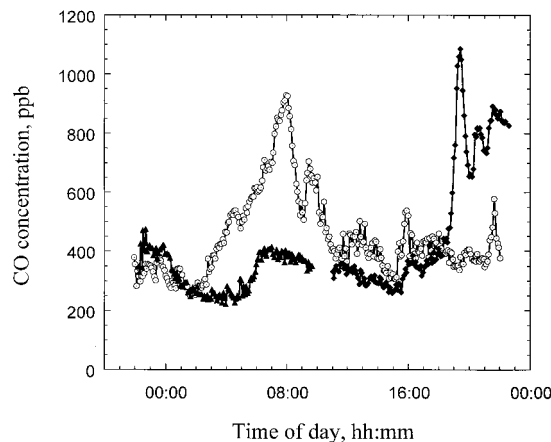


Fig. 5. Three test runs of continuous CO monitoring in ambient laboratory air. A test run started on Friday, 9 March, 2001 (diamonds). An example spectrum in Fig. 2(a) corresponds to the last measurement of this run. A second test run started on Tuesday, 13 March, 2001 (open circles) and a third test run that commenced on 14 March, 2001 (triangles). Interval between consecutive measurements was 5 min.

Financial support of the work performed by the Rice group, and PSI was provided by the National Institutes of Health through grant 1R43HL64452-02-01A1. Support was also received from the National Aeronautics and Space Administration, the Institute for Space Systems Operations, the Texas Advanced Technology Program, the National Science Foundation, and the Welch Foundation. The work performed at Bell Laboratories was partially supported by DARPA/US ARO under contract number DAAD19-00-C-0096. R. Köhler acknowledges support from Deutsche Studienstiftung.

## References

1. F. Capasso, C. Gmachl, R. Paiella, A. Tredicucci, A. L. Hutchinson, D. L. Sivco, J. N. Baillargeon, A. Y. Cho, and H. C. Liu, "New frontiers in quantum cascade lasers and applications," *IEEE J. Sel. Top. Quantum Electron.* **6**, 931–946 (2000).
2. C. Gmachl, F. Capasso, R. Köhler, A. Tredicucci, A. L. Hutchinson, D. L. Sivco, J. N. Baillargeon, and A. Y. Cho, "The senseability of semiconductor lasers," *IEEE Circuits Devices Mag.*, May 2000, pp. 10–18.
3. R. Köhler, C. Gmachl, A. Tredicucci, F. Capasso, D. L. Sivco, S. N. G. Chu, and A. Y. Cho, "Single-mode tunable, pulsed, and continuous wave quantum-cascade distributed feedback lasers at  $\lambda \sim 4.6\text{--}4.7 \mu\text{m}$ ," *Appl. Phys. Lett.* **76**, 1092–1094 (2000).
4. A. A. Kosterev, F. K. Tittel, R. F. Curl, R. Köhler, C. Gmachl, F. Capasso, D. L. Sivco, and A. Y. Cho, "Transportable automated ammonia sensor based on a pulsed thermoelectrically cooled QC-DFB laser," *Appl. Opt.* **41**, 573–578 (2002).
5. K. Namjou, S. Cai, E. A. Whittaker, J. Faist, C. Gmachl, F. Capasso, D. L. Sivco, and A. Y. Cho, "Sensitive absorption spectroscopy with a room-temperature distributed-feedback quantum-cascade laser," *Opt. Lett.* **23**, 219–221 (1998).
6. A. A. Kosterev, F. K. Tittel, C. Gmachl, F. Capasso, D. L. Sivco, J. N. Baillargeon, A. L. Hutchinson, and A. Y. Cho, "Trace-gas

- detection in ambient air with a thermoelectrically cooled, pulsed quantum-cascade distributed feedback laser," *Appl. Opt.* **39**, 6866–6872 (2000).
7. L. S. Rothman, C. P. Rinsland, A. Goldman, S. T. Massie, D. P. Edwards, J.-M. Flaud, A. Perrin, C. Camy-Peyret, V. Dana, J.-Y. Mandin, J. Schroeder, A. McCann, R. R. Gamache, R. B. Wattson, K. Yoshino, K. V. Chance, K. W. Jucks, L. R. Brown, V. Nemtchinov, and P. Varanasi, "The HITRAN Molecular Spectroscopic Database and HAWKS (HITRAN Atmospheric Workstation): 1996 Edition," *J. Quant. Spectrosc. Radiat. Transfer* **60**, 665–710 (1998).
  8. A. A. Kosterev, A. L. Malinovsky, F. K. Tittel, C. Gmachl, F. Capasso, D. L. Sivco, J. N. Baillargeon, A. L. Hutchinson, and A. Y. Cho, "Cavity ringdown spectroscopic detection of nitric oxide with a continuous-wave quantum-cascade laser," *Appl. Opt.* **40**, 5522–5529 (2001).
  9. Courtesy of E. Dlugokencky, National Oceanic and Atmospheric Administration, Climate Monitoring and Diagnostic Laboratory, Boulder, Colo.
  10. T. Töpfer, K. P. Petrov, Y. Mine, D. Jundt, R. F. Curl, and F. K. Tittel, "Room-temperature mid-infrared laser sensor for trace gas detection," *Appl. Opt.* **36**, 8042–8049 (1997).